

MIMO Measurements at high UE Velocity with variable eNB Antenna Column Separation

Ola Bidhan¹, Michael Einhaus¹, Juergen Beyer², Kevin Kaiser²

¹ Leipzig University of Applied Sciences, Germany, ola.bidhan@htwk-leipzig.de, michael.einhaus@htwk-leipzig.de

² Deutsche Telekom, Germany, juergen.beyer@telekom.de, kevin.kaiser@telekom.de

Abstract— In order to provide sufficient data rates in high mobility scenarios, LTE mobile radio networks along railways must be deployed at high carrier frequencies with large bandwidth, where typically 4x4 Multiple-Input Multiple-Output (MIMO) is used. It is a well known fact that the performance of 4x4 MIMO typically decreases as mobile user velocity increases. However, reducing the correlation within the MIMO radio channel may lead to reduced degradation of the MIMO performance. To verify this effect, the distance between two single-column antennas on the evolved NodeB (eNB) side has been varied between 0.2 m and 15 m, and comprehensive drive tests have been conducted at 120 km/h. It has been observed that with 3 m antenna column separation, the achieved throughput gain compared to 0.2 m column separation is around 20 % and that it does not further improve with additional separations, although the utilization of three MIMO spatial layers further increases.

Index Terms — LTE, MIMO measurements, variable eNB antenna separation, high UE velocity.

I. INTRODUCTION

The demand for higher data rates is a common requirement for most mobile users, and mobile network operators are therefore challenged to fulfill this customer demand. In urban areas with dense radio access network deployments and a wide range of radio frequencies, LTE mobile radio access is readily available at velocities of up to 120 km/h. In such scenarios, the bandwidth of multiple LTE cells operating in different frequency bands are typically combined by means of carrier aggregation.

In rural areas, on the other hand, this is not always the case. Dense deployments of LTE cells at 2.6 GHz or 3.5 GHz cannot be expected everywhere due to the insufficient coverage area of radio cells at these frequencies.

Under these conditions, the situation in rural areas becomes quite unsatisfying along motorways and railway tracks. Trains in particular yield a high density of radio

network users, resulting in large data rate demands within a very limited area.

Due to the limited available bandwidth in such scenarios, it is therefore essential to increase the spectral efficiency by means of MIMO transmission schemes. Multi-antenna transmission and reception has therefore been introduced from the very beginning in Release 8 for LTE by the 3rd Generation Partnership Project (3GPP). For the operation at 1.8 GHz and above, 4x4 MIMO is currently state of the art and typically supported by both evolved NodeB (eNB) and user equipment (UE) for downlink transmissions. The possibility to use up to four spatial layers can therefore significantly increase the achievable data rates compared to 2x2 MIMO or Single-Input Single-Output (SISO) transmission schemes.

Although 4x4 MIMO with up to four spatial layers provides significantly higher peak spectral efficiencies than 2x2 MIMO, its performance will decrease as UE velocity increases due to channel estimation and precoder reporting accuracy issues [1],[2]. The closed loop MIMO transmission scheme is typically used in LTE since it is the most efficient MIMO mode in terms of achievable data rate [3]. For downlink transmissions, the delay between the estimation of MIMO parameters based on channels measurements on UE side and the first reception of data transmitted by employing the corresponding transmission parameters comprises typically 8 ms. For moderate UE velocities, this is sufficient, but not for high-speed trains due to the low coherence time of the radio channel at high velocities. Consequently, the estimated MIMO parameters do not match the actual radio channel a few milliseconds later. The parameters comprise the precoding matrix indicator (PMI) and the rank indicator (RI). The first addresses a specific spatial precoder from a code book and the latter describes the number of spatial layers that can be used for data transmissions [4].

The basic concept behind the measurement campaign presented in this paper is to improve the robustness and spectral efficiency of the 4x4 MIMO transmission performance in high mobility scenarios by reducing the correlation within the MIMO channel matrix between eNB and UE. In order to achieve this, the eNB antenna element separation has to be enhanced by increasing the eNB antenna columns distance.

For the measurement campaign, two single-column X-pol antennas have been mounted on the rooftop of a high building close to a motorway and the distance between both eNB antennas has been varied between 0.2 m and 15 m. The UEs used during the measurement campaign were located in a measurement van that was driving on the motorway with a constant velocity of 120 km/h. The scenario was chosen with the intention of maximizing the line-of-sight (LOS) probability between eNB and UE since this is expected to be representative for typical deployments at motorways and railways.

The measurement setup on the eNB side as well as on the UE side and the measurement area are described in Section II. The basic steps of the data processing are introduced in Section III, and the results are discussed in Section IV.

II. MEASUREMENT SCENARIO AND SETUP

A. Setup at eNB and UE Side

The LTE measurements were performed at 1.8 GHz with a downlink bandwidth of 20 MHz supporting 4x4 MIMO with up to four spatial layers. The site used for this measurement is located on a grain silo. For the trials, two identical single-column X-pol antennas with two ports (Commscope, HBX-6513DS-VTM) [5] were installed on the flat rooftop of the silo at a height of 32 m above ground level. The combination of two of these antennas allows for transmission and reception on four antenna ports (4T4R) overall, thereby facilitating the diversity in downlink and uplink direction.



Figure 2.1: eNB antenna configuration and view to the motorway. The antenna separation s_{ant} is varied between 0.2 m and 15 m.

One antenna was mounted at a fixed position, while the other antenna was installed on a portable antenna pole to vary the distance between both antennas. The distance between the antennas is equivalent to the column separation of a dual column antenna. During the measurement campaign, the antenna columns were separated by distances s_{ant} of 0.2 m (antenna cabinets side by side), 3 m, 8 m, 12 m, and 15 m.

The measurement setup comprises two UEs, where one UE generates traffic in the downlink direction and the other UE in the uplink direction by down- and uploading data from and to a server. The UEs were mounted on the side window of the measurement van. The measurement system that has been used is X-CAL from Accuver [6] which collects data from the UEs on transmission time interval (TTI) level. This corresponds to a time resolution of one millisecond in case of LTE.

B. Measurement Scenario

In order to evaluate the MIMO performance at high UE velocity, the measurements were performed on a motorway nearby the site at a speed of 120 km/h. The motorway runs in a north-south direction through a rural area with little vegetation on both sides. The LOS path between the UEs and the eNB antennas is not obstructed. The length of the motorway section with contiguous LOS used for the data analysis is approximately 2.5 km and the maximum distance to the eNB antenna site is 2.9 km as shown in Figure 2.2.

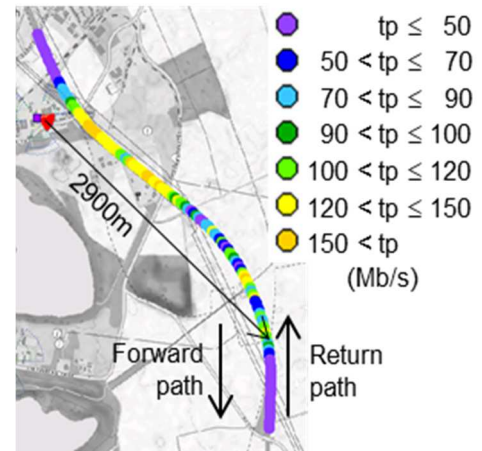


Figure 2.2: Site location (red symbol: eNB) and downlink throughput (tp) over the measurement route. The contiguous LOS part of the route ends at a 2.9 km distance.

For optimal coverage along the measurement route, the horizontal main lobe direction of both antennas was set to 120° (south-eastern direction), and an electrical downtilt of 2° was configured. In order to mitigate the impact of inter-cell interference, neighbor cells operating in the same frequency band were furthermore switched off during the measurement campaign.

For the sake of data reliability, six drive tests have been carried out for each considered antenna separation: three runs in north-south direction starting close to the site, denoted forward path (see Figure 2.2), and three runs in south-north direction starting at a maximum distance of 2.9 km from the site, denoted return path.

III. DATA ANALYSIS

The measurements campaign was conducted in a commercial mobile radio network where radio resources are typically shared between active UEs. In order to derive estimates for the maximum achievable throughput for the evaluated UEs, the throughput that has been observed during the measurement has been normalized to the assumption of full resource allocation for that UE, with the corresponding resource utilization. The procedure is described by the following equation:

$$Tput_{norm} = \frac{N_{RB,Band} \cdot Tput_{TBS}}{N_{RB,Sched}} \quad (1)$$

The TTI-based throughput ($Tput_{TBS}$) is calculated over the transport blocks (TBs) that have a positive Cyclic Redundancy Check (CRC) flag. $N_{RB,Sched}$ is the number of resource blocks (RBs) allocated to the UE within a TTI, and $N_{RB,Band}$ is the number of overall available RBs for data transmissions. In an LTE deployment with 20 MHz system bandwidth, as evaluated during the measurement campaign, $N_{RB,Band}$ is 100.

The Accuver measurement system delivers data concerning the observed key performance indicators (KPIs) on TTI-level (one sample per millisecond) or on an average-per-second basis, whereby averages of the observed KPIs are reported. Due to the high resolution in time domain, the TTI-level data are generally more favorable since these enable a more precise throughput normalization. However, since the entire measurement duration was approximately four hours, the TTI-level evaluation would result in a very large amount of data. For some drive tests during the measurement campaign, the throughput evaluation of the TTI-level data set has therefore been compared with the throughput evaluation of a corresponding average-per-second data set. Since the differences were rather small and negligible, the average-per-second measurement data has been used for the evaluation due to practical reasons.

Due to several effects, such as for example trucks obstructing the LOS path, the data that have been collected during different runs, partially deviate. To attain a high level of reliability, a two-step data selection process has been conducted based on generated plots as presented in Figure 3.1 which shows the downlink throughput of all three runs of the forward path for one antenna separation. Only the contiguous LOS part of the drive tests is used for the data analysis. In the first step, those two runs having the most matching graphs are selected. In Figure 3.1 these correspond to the red (r2) and green (r3) graphs. In the second step, the parts of the graphs, where the selected two runs exhibit significant throughput deviations, are discarded as well. A significant deviation between the red (r2) and the green (r3) graph can be seen at the beginning of the LOS region. After this process, the results of these two runs are highly consistent in terms of observed throughput.

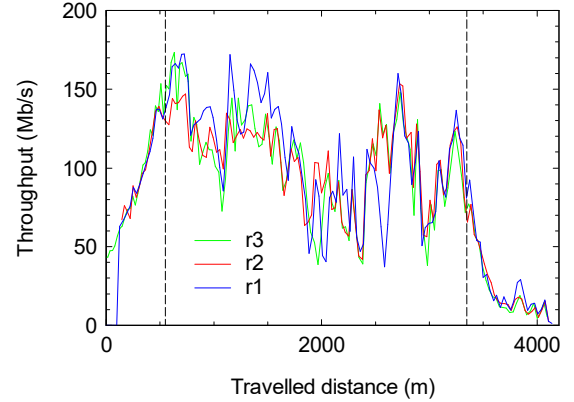


Figure 3.1: The downlink throughput over the traveled distance of all three runs of the forward path for $s_{ant} = 3m$. LOS is given for the part of the route between the two black dashed lines. This part is evaluated.

For the statistical evaluation, the data samples of the two runs that have been selected based on the postprocessing described above are joined into a single data set. This is done separately for both forward and return path. The described data selection process is furthermore applied for both down- and uplink measurement data. Hence, four data sets will be available at the end of these procedures; downlink and uplink evaluation for the forward path, and downlink and uplink evaluation for the return path.

IV. RESULTS

The focus of the investigation is on the downlink performance evaluation. The uplink is regarded additionally with respect to the impact of the antenna column separation on the cell coverage. For simplicity, the term ‘throughput’ will be used instead of ‘normalized throughput’ in the following discussion.

A. Downlink

For the given scenario with eNB antennas 32 m above ground level and LOS conditions on the measurement route, a dominant propagation path could be assumed with only minor contributions of reflected parts. Figure 4.1 shows the cumulative distribution function (CDF) of the downlink throughput achieved by 2x4 MIMO (1 single X-Pol antenna) and by 4x4 MIMO (2 single X-pol antennas side by side). This is done to check if there is any gain of 4x4 over 2x4 MIMO in this LOS dominated scenario. In the latter case, the antenna column separation s_{ant} was 0.2 m. The performance benefit of 4x4 over 2x4 MIMO is evident. For the median throughput, the gain is around 20 %, which is not much lower than the gain obtained from measurements in urban areas [7]. For the higher throughput, the gain of 4x4 MIMO decreases slightly. The median value of the throughput is around 110 Mb/s which is definitely immense for a UE moving at 120 km/h.

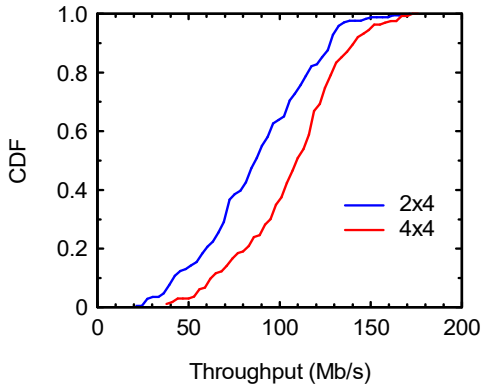


Figure 4.1: CDF of downlink throughput for 2x4 and 4x4 MIMO

In a typical mobile radio network deployment, the two antenna columns for the 4x4 MIMO configuration are enclosed side-by-side in a single antenna cabinet. This setup therefore serves as a baseline for the following analysis. All gains/losses are related to this setup with antenna separation $s_{ant} = 0.2$ m. For evaluating the impact of s_{ant} on the downlink throughput, the relative throughput difference $\Delta tput_{p,s}$ is computed at specific percentiles of the throughput distribution according to following equation:

$$\Delta tput_{p,s} = \frac{tput_{p,s} - tput_{p,0}}{tput_{p,0}} \quad (2)$$

The index p represents the evaluated statistical parameter of the downlink throughput distribution (10th percentile, 90th percentile, and average) and index s symbolize the antenna column separation, e.g. $s = 0.2$ m means the antennas are side by side.

Figure 4.2 illustrates $\Delta tput$ for the predefined antenna separations of the return path. The gain of the average throughput (red markers in Figure 4.2) is about 20% for $s_{ant} = 3$ m and it does not grow further with increasing s_{ant} . Higher throughput values according to the 90th percentile (black markers in Figure 4.2) benefits much more from larger s_{ant} values than lower throughput values as indicated by the 10th percentile (blue markers in Figure 4.2).

The essential idea behind the measurement campaign was to reduce the correlation within the MIMO radio channel established between eNB and UE antennas by increasing the eNB antenna column separation [8]. To verify this concept, the utilization of scheduled MIMO layers has been analyzed for the forward path as shown in Figure 4.3. The figure evaluates the spatial rank of the downlink MIMO channel as reported from the UE to the eNB.

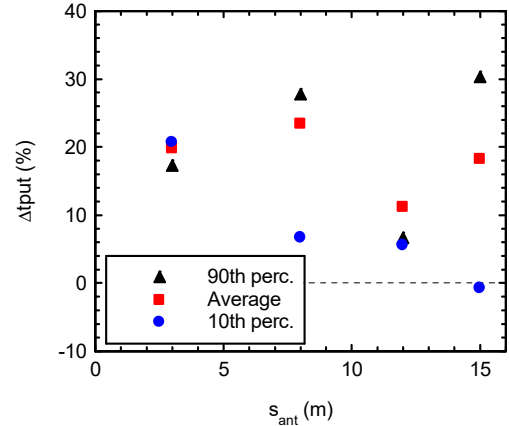


Figure 4.2: The downlink throughput difference $\Delta tput$ of the return path for different antenna separations s_{ant} .

Around 15 % of the collected data samples indicate a utilization of three spatial layers (Rank 3) at $s_{ant} = 0.2$ m. This ratio increases up to 40 % with an antenna separation $s_{ant} = 15$ m. The evaluation of the return path have revealed similar results. This implies that by increasing the antenna separation s_{ant} from 0.2 m to 15 m, the utilization of three spatial layers (Rank 3) is more than doubled, which verifies that the radio channel correlation decreases significantly with increasing eNB antenna column separation.

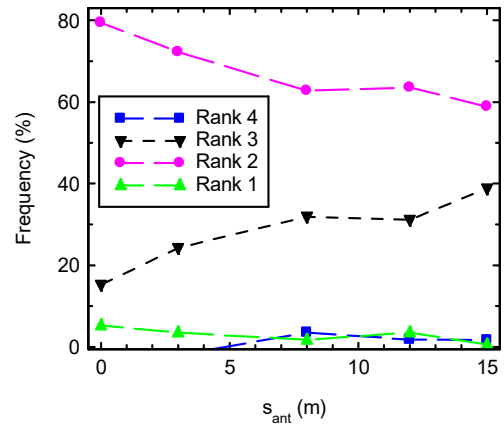


Figure 4.3: The distribution of used spatial MIMO layers as indicated by the reported rank on the forward path depending on antenna separations s_{ant} .

However, no throughput increase has been observed based on the increased MIMO channel rank. This is assumed to be based on the fact that the modulation order decreases with increasing antenna separation s_{ant} . With $s_{ant} = 0.2$ m, the 256QAM utilization is 40 %, which is reduced to only 20 % with $s_{ant} = 15$ m which compensates the effect of the increased MIMO rank on the observed throughput. Reasons for these observations are expected to be a result of interference between the spatial layers and distribution of the overall transmit power on the spatial layers in the eNB.

B. Uplink

In conjunction with throughput improvements in the downlink directions, increasing the eNB antenna column separation might also contribute to increasing the coverage area of a cell. Since the uplink coverage basically determines the cell size, the uplink throughput has therefore been investigated as well. Figure 4.4 shows the corresponding results depending on the downlink coupling loss L_c between UE and eNB, assuming the downlink and uplink coupling loss correspond to each other. The coupling loss has been determined according to:

$$L_c = P_{sc} - \text{RSRP} \text{ (dB)} \quad (2)$$

Where P_{sc} is the transmission power per subcarrier on the eNB side and Reference Signal Received Power (RSRP) is the average received power of the cell-specific reference signals (CRS) in the UE. To determine the coverage gain, the part of the graph (Figure 4.4) with the approximately linear throughput decrease ($L_c > 65$ dB) is considered. For a specific throughput, the associated L_c is identified for $s_{ant} = 0.2$ m (reference) and a second s_{ant} . The coverage gain corresponds to the RSRP difference between both s_{ant} values. No coverage gain is obtained for $s_{ant} = 3$ m, whereas the coverage gain with $s_{ant} = 15$ m is up to approximately 4 dB. Indicating that a significant coverage gain can be obtained only with a quite large antenna separation which, however, is not realistic for most sites.

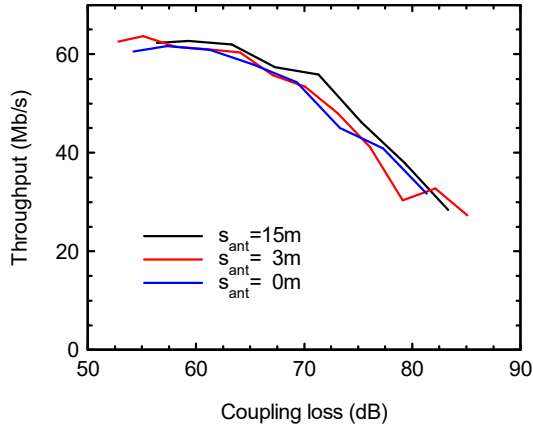


Figure 4.4: The uplink throughput depending on the coupling loss between UE and eNB and antenna column separation s_{ant} . The plot shows non-overlapping piecewise averages in 3dB intervals.

V. SUMMARY

Comprehensive measurements in a commercial LTE cell at 1.8 GHz have been performed to investigate the impact of eNB antenna column separation on the 4x4 downlink MIMO performance and on the uplink coverage. For that purpose, an eNB was equipped with two single-column X-Pol antennas, and their separation was varied between 0.2 m and 15 m. The measurements were performed on a nearby motorway at 120 km/h under LOS conditions.

The investigation shows that the 4x4 MIMO throughput increases by roughly 20% with increasing antenna column separation from 0.2 m to 3 m and remains on that level when the eNB antenna column separation further increases. The utilization of three spatial layers (Rank 3) rises continuously from 20% at 0.2 m antenna column separation to 40 % at 15 m antenna column separation which verifies the MIMO channel correlation reduction by increasing the distance between both eNB single-column antennas. However, the 256QAM utilization exhibits the opposite trend and diminishes with increasing antenna column separation, which compensates the theoretical throughput gain of higher rank utilization.

According to the uplink measurements, a significant coverage gain can only be expected with more than 12 m distance between the eNB antennas in the evaluated scenario.

ACKNOWLEDGMENT

The authors would like to thank the German Federal Network Agency, Section 414, for supporting this campaign.

REFERENCES

- [1] Kamran Arshad, LTE System Level Performance in the Presence of CQI Feedback Uplink Delay and Mobility, University of Greenwich, United Kingdom, 2015. Accessed: August 18, 2021.
- [2] Rudi Abi, Compensating for CQI Aging By Channel Prediction: The LTE Downlink, Fraunhofer Institute for Telecommunications Heinrich Hertz Institute. Berlin. 2012. Accessed: August 18, 2021.
- [3] K. Werner, J. Furukskog, M. Rieback, and B. Hagerman, "Antenna configuration for 4x4 MIMO in LTE-Field measurements", IEEE 71st Vehicular technology conference, 2010
- [4] Evolved Universal Terrestrial Radio Access (E-UTRA); Physical layer procedures, 3GPP TS 36.213. [Online]. Available: https://www.etsi.org/deliver/etsi_ts/136200_136299/136213/17.01.00_60/ts_136213v170100p.pdf
- [5] CommScope, CA, USA. HBX-6513DS-VTM (2022). Accessed: September 17, 2021. [Online]. Available: <https://de.commscope.com/globalassets/digizuite/262534-p360-hbx-6513ds-vtm-external.pdf>
- [6] Accuver, XCAL "PC based Advanced 5G Network Optimization Solution," <https://www.accuver.com/>. (accessed: May 17, 2021). [Online]. Available: <https://www.accuver.com/sub/products/view.php?idx=6>
- [7] K. Kaiser, „Empirical investigation of the MIMO performance at high UE velocity for varying eNB antenna column separation”, Bachelor-Thesis (written in German), Leipzig University of Applied Sciences, Leipzig, Germany, 2021.
- [8] Christian Schneider et al, "Characterization of Urban Radio Channels and Base Station Antenna Correlation at the 3.75GHz Band", IEEE vehicular technology conference, 2021
- [9] Requirements for Further Advancements for Evolved Universal Terrestrial Radio Access (EUTRA) (LTE-Advanced), 3GPP TR 36.913, 2014. [Online]. Available: <http://www.3gpp.org/DynaReport/36913.htm>